Available online at www.sciencedirect.com
SCIENCE DIRECT®
Agricultural and Forest Meteorology 124 (2004) 219–236
AGRICULTURAL AND FOREST METEOROLOGY
www.elsevier.com/locate/agrformet

A model of the production and transport of CO_2 in soil: predicting soil CO_2 concentrations and CO_2 efflux from a forest floor

R.S. Jassal*, T.A. Black, G.B. Drewitt, M.D. Novak, D. Gaumont-Guay, Z. Nesic

Faculty of Agricultural Sciences, University of British Columbia, 2357 Main Mall, Vancouver, BC, Canada V6T 1Z4

Received 2 June 2003; received in revised form 26 January 2004; accepted 29 January 2004

Abstract

A process-based model of the transport of heat and water in the soil and surface energy balance components is extended to include production of CO_2 from heterotrophic (microbial decomposition) and autotrophic (root) respiration, and transport of the resulting CO_2 in both the gaseous and liquid phases. The production of CO_2 is determined by the amount and type as well as distribution in the soil profile of organic matter and roots, and their respective first-order rate constants. Influences of soil water and temperature are considered through their effects on respiration, CO_2 diffusivities and chemical equilibria among various C species in the soil–solution–air continuum. Also included is CO_2 uptake by plant roots associated with root water uptake.

Model calculations, using independently determined parameters, are compared with measurements of soil CO_2 concentrations and chamber-measured forest floor fluxes in a second-growth 54-year-old Douglas-fir forest located on the east coast of Vancouver Island, Canada. Measured and modeled forest floor CO_2 effluxes and soil CO_2 concentration profiles, as well as soil water contents and temperatures showed good agreement. The efflux was most sensitive to soil temperature, and the influence of soil water content was relatively small. In this rapidly draining soil, the CO_2 efflux, at time scales as small as half-hour, was very well approximated by the total production of CO_2 in the soil profile, even during and after rainfall, which significantly increases soil water content. This is because CO_2 diffusion in this forest soil is relatively rapid compared to changes in the rates of CO_2 production. In this podzolic soil ecosystem with low soil pH, liquid-phase diffusion appears to play a minor role in CO_2 transport. High soil CO_2 concentrations, up to 10,000 μmol mol^{-1} in summer and 6000 μmol mol^{-1} in winter, and a positive downward gradient at the 1 m depth indicate some CO_2 sources associated with very low CO_2 diffusivity at deeper depths.

Keywords: Soil respiration; Soil CO_2 efflux; Soil CO_2 concentration; Forest soil; Soil temperature; Soil water content

1. Introduction

Soil CO_2 efflux represents 40–80% of the forest ecosystem respiration (Janssens et al., 2001; Law et al., 1999) and is therefore one of the major processes to consider when determining the carbon balance of forests. However, spatial heterogeneity of local site characteristics and the temporal variability of factors affecting CO_2 production and transport all conspire against any simple description of these processes (Rayment and Jarvis, 2000; Drewitt et al., 2002). Furthermore, reliable field measurements of fluxes from soils are very difficult to obtain (Norman et al., 1997). While there are different types of chamber systems to measure gas fluxes at the soil surface (Livingstone and Hutchinson, 1995), there is no stan-

* Corresponding author. Tel.: +1-604-822-9119; fax: +1-604-822-2184.
E-mail address: rachhpal.jassal@ubc.ca (R.S. Jassal).

0168-1923/$ – see front matter © 2004 Elsevier B.V. All rights reserved.
doi:10.1016/j.agrformet.2004.01.013

Nomenclature

b	Clapp and Hornberger parameter relating soil water content and potential
C_a	CO_2 concentration in the air at a reference height (mol m^{-3})
C_G	CO_2 concentration in soil air (mol m^{-3} soil air)
C_h	heat capacity of soil (J m^{-3} K^{-1})
C_L	CO_2 concentration in soil water (mol m^{-3} soil water)
C_{soil_L}	labile fraction of soil organic carbon (mol m^{-3} whole soil)
C_{soil_R}	resistant fraction of soil organic carbon (mol m^{-3} whole soil)
C_T	total CO_2 concentration in soil liquid and gaseous phases (mol m^{-3} whole soil)
D	molecular diffusivity (m^2 s^{-1})
D_{CG}	CO_2 diffusivity in soil air (m^2 s^{-1})
D_G	CO_2 diffusivity in air (m^2 s^{-1})
D_L	CO_2 diffusivity in water (m^2 s^{-1})
D_{T_1}	gas diffusivity at temperature T_1
D_{T_2}	gas diffusivity at temperature T_2
D^*_{CL}	effective diffusivity (diffusion + dispersion) of CO_2 in soil water (m^2 s^{-1})
E	stand evapotranspiration (kg m^{-2} s^{-1})
f_G	gaseous-phase tortuosity (soil impedance factor for gaseous-phase diffusion)
f_L	liquid-phase tortuosity (soil impedance factor for liquid-phase diffusion)
F_G	flux due to gaseous-phase CO_2 diffusion (mol m^{-2} s^{-1})
F_L	flux due to liquid-phase CO_2 diffusion (mol m^{-2} s^{-1})
F_{root}	fine root biomass density (kg m^{-3})
g	acceleration due to gravity (9.8 m s^{-2})
G_S	soil heat flux density (W m^{-2})
$k_{C_{root}}$	rate constant of CO_2 production from coarse root respiration (s^{-1})
$k_{F_{root}}$	rate constant of CO_2 production from fine root respiration (s^{-1})
k_L	rate constant of CO_2 production from labile fraction of soil organic C (s^{-1})
k_R	rate constant of CO_2 production from resistant fraction of soil organic C (s^{-1})
K	equilibrium constants as defined in Table 1
K_L	unsaturated hydraulic conductivity of soil (kg s m^{-3})
K_{LT}	non-isothermal liquid water conductivity (kg m^{-1} s^{-1} K^{-1})
K_{T_1}	equilibrium constant at temperature T_1
K_{T_2}	equilibrium constant at temperature T_2
K_V	water vapor conductivity (kg s m^{-3})
K_{VT}	non-isothermal water vapor conductivity (kg m^{-1} s^{-1} K^{-1})
K^*_T	apparent thermal conductivity of soil (W m^{-1} K^{-1})
L	latent heat of vaporization (J kg^{-1})
$M_{C_{root}}$	coarse root mass density in soil (mol C m^{-3})
$M_{F_{root}}$	fine root mass density in soil (mol C m^{-3})
P	barometric pressure (Pa)
q_w	liquid water flux (kg m^{-2} s^{-1})
r_a	surface boundary layer (aerodynamic) resistance in air (s m^{-1})
R	gas constant (8.31 J mol^{-1} K^{-1})
R_C	actual rate of total soil CO_2 production (mol m^{-3} s^{-1})
$R_{C(opt)}$	optimum rate of total soil CO_2 production (mol m^{-3} s^{-1})

S_{CO_2}	CO_2 mole fraction in soil air (mol mol^{-1} moist air)
S_w	rate of root water uptake in soil (kg m^{-3} soil s^{-1})
s_{w_i}	fraction of the total water uptake that takes place in the *i*th layer
t	time (s)
T	temperature (K)
U_C	sink term of soil C removed in the uptake of water by roots (mol m^{-3} s^{-1})
z	depth in soil (m)

Greek symbols

$\alpha(T)$	soil respiration reduction coefficient due to temperature effects
$\alpha(\theta)$	soil respiration reduction coefficient due to soil water content effects
ΔH	standard molar enthalpy change (kJ mol^{-1})
ε	air-filled porosity of soil ($\theta_S - \theta$) (m^3 m^{-3} whole soil)
ε_R	relative air-filled porosity of soil (ε/θ_S)
θ	volumetric soil water content (m^3 m^{-3} whole soil)
θ_{awf}	plant available soil water fraction (m^3 m^{-3} whole soil)
θ_{fc}	volumetric soil water content at field capacity (m^3 m^{-3} whole soil)
θ_R	relative water-filled porosity of soil (θ/θ_S)
θ_S	total soil porosity or saturation soil water content (m^3 m^{-3} whole soil)
θ_{wp}	volumetric soil water content at wilting point (m^3 m^{-3} whole soil)
λ	water dispersion coefficient in soil (m)
ρ_w	density of water (kg m^{-3})
ψ	soil water matric potential (J kg^{-1}) (1 J kg^{-1} = 0.1 m of water column)

dard approach that is suitable for all situations. Similarly, eddy correlation flux measurements, especially below forest canopies, are often marred by relatively low wind speeds (Drewitt, 2002).

Several studies have developed empirical relationships between soil CO_2 effluxes and environmental variables (Bunnell et al., 1977; Nakane, 1994). These studies have shown that efflux is primarily a function of soil temperature (Raich and Schlesinger, 1992). Soil moisture also influences soil respiration. Bunnell et al. (1977) assumed effects of soil water content and temperature on soil respiration to be multiplicative and developed a relationship that worked well at moderate soil water contents and temperatures. Hanson et al. (1993) developed an empirical relationship to predict CO_2 efflux by relating it to soil temperature, soil water content and the coarse mineral soil fraction. Burton et al. (1998) showed that soil moisture deficits decreased root respiration by up to 17%, and Goulden et al. (1996) showed that heterotrophic respiration decreased more than autotrophic respiration during extended drought in a temperate forest.

Two major processes determine CO_2 efflux from the soil: the production of CO_2 in the soil, and its transport within the soil and transfer across the soil surface to the atmosphere. In a process-based model both of these processes must be accounted for. Simunek and Suarez (1993) developed such a model of CO_2 production and transport in soil that included flow equations for soil water and heat, and their effect on microbial and root respiration. Their model included a large number of soil processes, including the effect of osmotic soil water potential on plant transpiration and the effect of temperature on root growth. Fang and Moncrieff (1999) presented a model of the production and transport of soil CO_2 without soil water and heat transport, with model parameters estimated with a multidimensional optimization method using site-specific information (Moncrieff and Fang, 1999).

The aim of this study is to describe a simple CO_2 production scheme and combine it with the simultaneous transport of soil water, heat and CO_2 in the soil. The modeled soil CO_2 concentrations and forest floor CO_2 effluxes as well as soil temperatures and water

contents, using model parameters from independent measurements, are compared with measurements in a 54-year-old Douglas-fir stand located on the east coast of Vancouver Island, Canada. The results are discussed in terms of the influences of soil variables on soil CO_2 effluxes and soil CO_2 concentrations with a special emphasis on the relative importance of production versus transport of CO_2 in determining the efflux.

2. Model description

2.1. Transport of soil heat and water

We have developed a physically based multi-layer numerical model to determine the coupled transport of heat and water in the soil and in the soil–atmosphere boundary layer (Jassal et al., 2003). Using inputs of standard weather data and initial soil conditions, the model is capable of predicting the soil surface energy balance components as well as water content and temperature profiles in the soil. Here we extend this model to include heterotrophic (microbial decomposition) and autotrophic (root) respiration and transport of the resulting CO_2 in both the gaseous and liquid phases. For brevity, only the equations describing the conservation and transport of energy and water in soil are reproduced here (see Jassal et al. (2003) for details). The vertical flow of soil water can be described by the following form of the Richards equation:

$$\frac{\partial\theta}{\partial t} = \frac{1}{\rho_w}\frac{\partial}{\partial z}\left[(K_L + K_V)\frac{\partial\psi}{\partial z} - gK_L + (K_{LT} + K_{VT})\frac{\partial T}{\partial z}\right] - \frac{S_w}{\rho_w} \quad (1)$$

where the first, second and third terms in the square brackets describe liquid and vapor transport in response to the soil water matric potential gradient, downward movement of liquid water due to gravity, and liquid and vapor transport in response to the soil temperature gradient, respectively. S_w is the rate of water uptake by plant roots. All symbols are defined in the Nomenclature.

The soil heat flow equation in which lateral transport is absent and advection of heat as a result of the mass flow of water is neglected can be written as

$$\frac{\partial T}{\partial t} = \frac{1}{C_h}\frac{\partial}{\partial z}\left[K_T^*\frac{\partial T}{\partial z} + LK_V\frac{\partial\psi}{\partial z}\right] \quad (2)$$

where the first term in the square brackets describes conduction and latent heat transport due to the temperature gradient and the second term describes latent heat transport associated with water vapor transport driven by soil water matric potential gradient.

Water uptake by the trees is distributed over all (n) layers of the soil profile, based on the amount of fine roots (F_{root}) and available water fraction (θ_{awf}) in the respective layers. Accordingly, the fraction of the total water uptake that takes place in the ith layer is obtained using (Campbell and Norman, 1998)

$$s_{w_i} = \frac{F_{root_i}\theta_{awf_i}}{\sum_{i=1}^{n} F_{root_i}\theta_{awf_i}} \quad (3)$$

where $\theta_{awf} = 1 - (1 + 1.3\theta_{av})^{-b}$, in which b is the Clapp and Hornberger parameter and $\theta_{av} = (\theta - \theta_{wf})/(\theta_{fc} - \theta_{wp})$ with the subscripts 'wp' and 'fc' referring to wilting point and field capacity, respectively.

2.2. CO_2 transport in soil

The CO_2 transport equation in a soil in which the lateral flow of CO_2 and its convection in the gas phase are neglected can be written as

$$\frac{\partial C_T}{\partial t} = \frac{\partial}{\partial z}\left[D_{CG}\frac{\partial C_G}{\partial z} + D_{CL}^*\frac{\partial C_L}{\partial z} - \frac{q_w}{\rho_w}C_L\right] + R_C - U_C \quad (4)$$

where the three terms in the square brackets refer to diffusion of CO_2 in the gaseous phase, diffusion and dispersion in the liquid phase, and transport of dissolved CO_2 by the mass flow of water, respectively, and q_w is the rate of liquid water flow given by

$$q_w = -K_L\frac{\partial\psi}{\partial z} + gK_L - K_{LT}\frac{\partial T}{\partial z} \quad (5)$$

R_C is the rate of CO_2 production resulting from heterotrophic and autotrophic respiration, and U_C is the CO_2 removed by root uptake of water and is given by

$$U_C = \frac{S_w C_L}{\rho_w} \quad (6)$$

where C_L is the CO_2 concentration in the liquid phase. In acidic to neutral soils, concentrations of HCO_3^- and CO_3^{2-} are very small, so that contribution of the solid phase to inorganic C dynamics in the liquid phase–gaseous phase continuum is negligible. In this

Table 1
C equilibria in the soil water–air continuum and values of equilibrium constants and enthalpy change (ΔH) at 25 °C (adapted from Stumm and Morgan (1981))

Equilibrium	Equilibrium constant	ΔH (kJ mol^{-1})
$CO_{2(L)} \rightleftharpoons CO_{2(G)}$	$K_1 = 1.2$ (dimensionless)	19.4
$CO_{2(L)} + H_2O \rightleftharpoons H_2CO_3$	$K_2 = 1.56 \times 10^{-3}$ (dimensionless)	−7.7
$H_2CO_3 \rightleftharpoons HCO_3^- + H^+$	$K_3 = 0.279$ (mol m^{-3})	−2.0
$HCO_3^- \rightleftharpoons CO_3^{2-} + H^+$	$K_4 = 4.68 \times 10^{-8}$ (mol m^{-3})	−3.5

case, total concentration of inorganic C in the liquid and gaseous phases, C_T, is given by

$$C_T = \theta C_L + \varepsilon C_G \quad (7)$$

where C_G is the CO_2 concentration in the gaseous phase and ε is the air-filled porosity of the soil. C_L and C_G are assumed to be in instantaneous local equilibrium. This assumption is reasonable because the rate of equilibration among C species is rapid compared to their rate of movement in soil under most conditions, so that there is no need to consider equilibrium kinetics. The important chemical equilibria in the soil–water–air continuum, which are used to describe C_T and different C species in soil solution, viz. $CO_{2(L)}$, H_2CO_3, HCO_3^-, CO_3^{2-} and $CO_{2(G)}$ in terms of the working variable C_L, are shown in Table 1. Thus

$$C_L = \left[1 + K_2 + \frac{K_2 K_3}{[H^+]} + \frac{K_2 K_3 K_4}{[H^+]^2}\right] \frac{C_G}{K_1} \quad (8)$$

where $[H^+]$ is the hydrogen ion concentration, K_1, K_2, K_3 and K_4 are the equilibrium constants as in Table 1, and C_G is related to the CO_2 mole fraction in the soil air, S_{CO_2}, using the ideal gas law as

$$C_G = \frac{P}{RT} S_{CO_2} \quad (9)$$

The effective diffusion-dispersion coefficient for CO_2 in the soil solution can be expressed as

$$D^*_{CL} = \theta f_L D_L + \frac{\lambda q_w}{\rho_w} \quad (10)$$

and the effective gaseous-phase diffusion coefficient as

$$D_{CG} = \varepsilon f_G D_G \quad (11)$$

where f_L and f_G are the liquid- and gaseous-phase diffusion impedance factors (tortuosities), respectively, with f_L for this sand to loamy sand soil approximated by θ (Tinker and Nye, 2000) and f_G given by Currie (1965) as

$$f_G = m\varepsilon^n \quad (12)$$

with constants m and n determined from measurements. According to Marshall (1959), $m = 1$ and $n = 0.5$. D_L and D_G are the standard diffusion coefficients of CO_2 in water and air and are 1.66×10^{-9} m^2 s^{-1} (Robinson and Stokes, 1959) and 1.39×10^{-5} m^2 s^{-1} (Pritchard and Currie, 1982), respectively at 20 °C. The water dispersion coefficient, λ, for field scale applications is taken to be 0.1 m after Nielsen et al. (1986). The effect of temperature on the diffusion coefficients is estimated from

$$\frac{D_{T_2}}{D_{T_1}} = \left(\frac{T_2}{T_1}\right)^{\eta} \quad (13)$$

where η is roughly 1 for liquid diffusion and 1.75 for gaseous diffusion (Campbell, 1985). A potentially more significant effect may be on the equilibrium constants in Eq. (8), whose temperature influence is given by Harned and Davies (1943) as

$$\ln\left(\frac{K_{T_2}}{K_{T_1}}\right) = -\frac{\Delta H}{R}\left(\frac{1}{T_2} - \frac{1}{T_1}\right) \quad (14)$$

where ΔH is the standard molar enthalpy (kJ mol^{-1}) change for the reaction (Table 1).

2.3. CO_2 production in soil

Total soil organic matter content is divided into labile, C_{soil_L}, and resistant, C_{soil_R}, fractions with separate rate constants. The production of CO_2 from heterotrophic respiration is calculated as the sum of two first-order reactions as

$$R_{CS} = k_L C_{soil\_L} + k_R C_{soil\_R} \quad (15)$$

where k_L and k_R are the rate constants for labile and resistant soil carbon pools, respectively. Similarly, to calculate the production of CO_2 from autotrophic respiration, R_{CR}, roots are classified as fine and coarse, and the products of the rate constant and root mass density for the two classes are summed as follows (Chapman, 1979):

$$R_{CR} = k_{F_{root}} M_{F_{root}} + k_{C_{root}} M_{C_{root}} \quad (16)$$

where $M_{F_{root}}$ and $M_{C_{root}}$ are the fine and coarse root C mass densities, respectively, and $k_{F_{root}}$ and $k_{C_{root}}$ are the respective respiration rate constants. The total CO_2 production in the soil profile in optimum conditions, $R_{C(opt)}$, is then obtained by summing over all n layers, each of thickness Δz, as

$$R_{C(opt)} = \sum_{i=1}^{n}[(R_{CS}\Delta z)_i + (R_{CR}\Delta z)_i] \quad (17)$$

The effects of soil temperature on heterotrophic and autotrophic respiration are assumed to be similar, and the same is assumed for soil water content. These effects are assumed multiplicative, so that net CO_2 production is obtained from Eq. (17) as

$$R_C = \sum_{i=1}^{n}((R_{CS} + R_{CR})\alpha(T)\alpha(\theta)\Delta z)_i \quad (18)$$

where $\alpha(T)$ and $\alpha(\theta)$ are reduction coefficients with values between 0 and 1. We used an exponential function of soil temperature to evaluate $\alpha(T)$ as

$$\alpha(T) = Q_{10}^{(T-T_{ref})/10} \quad (19)$$

where the Q_{10} coefficient is the relative increase in respiration rate for a 10 °C increase in temperature.

To describe the influence of soil water content on soil CO_2 production, different relationships have been suggested (Tesarova and Gloser, 1976; Bunnell et al., 1977; Fang and Moncrieff, 1999). Generally, CO_2 production decreases at both very low and very high soil water contents. The reduction at very low soil water content is caused by inhibition of soil microbial and root metabolic activity, whereas at a very high soil water content, the reduction may be caused by lack of oxygen, or the accumulation of CO_2, as a result of the soil pore spaces being filled with water (Glinski and Stepniewski, 1985, p. 6). There is little or no change in CO_2 production with change in soil water content between low and high soil water contents (Bunnell et al., 1977; Tesarova and Gloser, 1976). Based on the above studies, we formulated the $\alpha(\theta)$ as a piecewise linear function of θ_R (relative water-filled porosity) as follows: for θ_R between 0 and 0.1, $\alpha(\theta)$ increases linearly from 0 to 0.6, for θ_R between 0.1 and 0.3, $\alpha(\theta)$ increases linearly from 0.6 to 1, for θ_R between 0.3 and 0.8, $\alpha(\theta) = 1$ and for θ_R between 0.8 and 1.0, $\alpha(\theta)$ decreases linearly from 1 to 0.5. We assumed that soil nitrogen does not limit soil microbial activity.

3. Materials and methods

3.1. Site description and soil characteristics

Measurements were made during 2000 and in 2002 in a 54-year-old Douglas-fir stand located about 10 km southwest of Campbell River (49°51′N, 125°19′W, 300 m above mean sea level), on the east coast of Vancouver Island, Canada. The site naturally regenerated after a forest fire in 1949, resulting in an almost homogeneous ∼130 ha stand. Tree density was about 1100 stems ha^{-1}, tree height was about 33 m and mean tree diameter at the 1.3 m height was 29 cm. Due to the closed canopy, light levels at the forest floor were generally very low.

The soil is a humo-ferric podzol having a pH of 5.4, underlain with a dense compacted till at a depth of 1 m and a surface organic layer between 1 and 5 cm thick. Below the organic layer is gravelly loamy sand to sandy loam with about 30% coarse fragments throughout the profile. The top 1 m of the mineral soil contained 11.6 kg organic carbon (OC) m^{-2}, which with 1.3 kg m^{-2} in the roots and 3 kg m^{-2} in the organic layer gave a total of 15.9 kg m^{-2} as an estimate of below-ground OC. An estimate for the above-ground OC was about 19 kg m^{-2} ground surface area. The forest floor supports a sparse understory consisting of herbs, ferns and mosses (Humphreys et al., 2003).

Soil volumetric water content was measured using four CSI (Model 615; Campbell Scientific Inc., Logan, UT) water content reflectometers at the 2–3, 10–12, 35–48 and 70–100 cm depths. In addition, 11 stations of time domain reflectometry (TDR) probes (Hook and Livingston, 1996) integrating the top 30 cm and the top 70 cm of the soil profile were manually measured monthly with a cable length tester (Model 1502B, Tektronix, Beaverton, OR) and used to account for the spatial variability in soil water content. Soil heat flux (G_S) was measured at three locations using soil heat flux plates (Model Middleton CN3, Carter-Scott Design, Victoria, Australia) buried at 2 cm below the soil surface, and corrected for heat storage changes in the overlying soil. Soil temperature measurements were made at the 2, 5 and 10 cm depths with chromel–constantan thermocouples. Half-hourly measurements of stand evapotranspiration (E) were made continuously using the eddy covariance technique (Humphreys et al., 2003).

3.2. Measurements of soil CO_2 effluxes, concentrations and diffusivities

Measurements of soil CO_2 efflux were made from mid-June to mid-December 2000 at six locations, 12–15 m from each other, using an automated chamber system. The system consisted of six dynamic closed (i.e. non-steady-state) transparent chambers and an infrared gas analyzer (IRGA) (Model LI-6262; LI-COR Inc., Lincoln, NE). Each chamber measured the efflux during a 4 min period each half hour. Details of the system are given in Drewitt et al. (2002).

CO_2 concentrations in the soil air were measured at two locations 50 m apart by drawing 10 cm^3 soil air samples out of probes buried at 2, 5, 10, 20, 50 and 100 cm depths. The probes were made of 30 cm long × 1.2 cm outer diameter (o.d.) perforated Dekaron tubing (Dekabon Type 1300; Dekaron, Furon Brands, Aurora, OH) coupled to a 0.3 cm o.d. stainless steel tube with a silicon rubber septum located just above the soil surface. Soil air samples were collected using a polyethylene 10 ml medical grade syringe inserted into the septum. Each sample was analyzed on-site by injecting it into a CO_2-free air stream passing through an LI-6262 IRGA. Sample concentration was determined from the ratio of the area under the concentration versus time curve to that obtained using a standard concentration (Drewitt, 2002).

From 25 September through 27 November 2002, soil CO_2 concentration at the 20 cm depth was continuously measured about 50 m away from the 2000 measurements but with a solid-state infrared CO_2 sensor (Model GMM221; Vaisala Oyj, Helsinki, Finland) with a 20 s time constant. The sensor was inserted into a horizontal hole made by auguring into the face of a soil pit, which was carefully back-filled to minimize the disturbance. Before installation, the sensor was covered with microporous Teflon tubing (Product Code 200-07; International Polymer Engineering Inc., Tempe, AZ) to protect it from soil particles and water. Microporous Teflon tubing excludes liquid water but allows free gas exchange. Preliminary runs indicated that the sensor body heated up to 4.5 °C higher than the ambient soil temperature within 30 min in a relatively dry soil, which affected the measurements. We found that having the sensor excitation (power applied) on for 5 min only during each hour resulted in very little heating with probe temperature always being within 0.2 °C of the ambient soil temperature at the same depth. The frequency of soil CO_2 concentration measurements was hourly. On 27 November, the sensor was excavated, brought to the laboratory and recalibrated. It was found that there was no change in the slope and offset.

We measured the gas diffusivity in undisturbed soil cores (length = 10 cm, internal diameter = 11 cm) under steady-state conditions using CO_2 as the diffusing gas. Soil cores were excavated from the 0–10, 10–20, 20–30, 30–40 and 40–50 cm depths from three locations. A high constant concentration (10,000 μmol mol^{-1} CO_2 in dry air) was maintained at the lower end of the soil column while the upper end was exposed to atmospheric CO_2 concentration. The diffusivity, D_{CG}, was calculated using $D_{CG} = F_e L/\Delta C_G$, where ΔC_G is the concentration gradient across the length, L, of the column and F_e the CO_2 efflux. It was obtained by measuring the rate of increase in CO_2 concentration over 2 min in a chamber placed over the upper end of the column. Air was circulated through the chamber and an infrared gas analyzer (Model LI-820; LI-COR Inc., Lincoln, NE) using a small diaphragm pump (Model TD-4X2N; Brailsford Co., NY).

3.3. Model inputs

The model inputs included soil characteristics, initial and boundary conditions. Soil characteristics were either measured or selected from the literature for reported measurements made for the most similar soil and environmental conditions. The average bulk density in the surface organic layer was 200 kg m^{-3}, while in the mineral soil it varied exponentially from 700 kg m^{-3} at the top to 1550 kg m^{-3} at the 1.5 m depth. Soil organic matter content was measured on soil samples taken from different depths using the loss on ignition method. Total soil organic matter was partitioned, following vanVeen and Paul (1981), Monreal et al. (1997) and Paul et al. (1999), into 'labile', 3%, and 'resistant', 45%, with the remaining as 'passive' which does not contribute to CO_2 production over the time scale of a few years. Soil organic matter content was 12.4% in the 0–10 cm mineral soil layer and decreased with increasing z, following a power function, to 1.7% in the 70–80 cm layer. The organic layer at the surface was partitioned into 25% labile

and 65% resistant and 10% passive (Muller, 2000). Following Wang et al. (2002), we used the soil organic matter decomposition rate constants being used in the CENTURY model, which were $1.0 \times 10^{-8}\,s^{-1}$ for k_L and $1.0 \times 10^{-9}\,s^{-1}$ for k_R.

Measurements in a 40-year-old Douglas-fir close to our experimental site showed fine roots to vary from 500 to 670 g dry matter m^{-2} (Kurz, 1989). Grier et al. (1981) observed fine root (excluding micorrhizae) biomass in a 23-year-old sub-alpine Douglas-fir to be 750 g dry matter m^{-2}. Based on the above studies, we used a total dry root biomass of 2500 g m^{-2} and divided it into 30% fine and 70% coarse fractions (Steele et al., 1997). Root-C was obtained by multiplying dry root mass by 0.45 (Muller, 2000). Both of these root fractions were then distributed in the soil profile with an exponential function described by Gerwitz and Page (1974). Following Moncrieff and Fang (1999) and Muller (2000), rate constants of 1.0×10^{-7} and $1.0 \times 10^{-8}\,s^{-1}$ were used for $k_{F_{root}}$ and $k_{C_{root}}$, respectively, in the simulations. Furthermore, based on Steele et al. (1997) and Kurz (1989) who showed fine root growth and mortality occurring concurrently and at almost equal rates, and for the sake of simplicity, we opted not to include fine root growth and mortality dynamics in our model. We used a Q_{10} of 2 for the bulk mineral soil and 4 for the surface organic layer (Witkamp, 1969).

The parameters K_S, ψ_e and b, required to calculate K_L and the $\psi - \theta$ relationship (for details see Jassal et al., 2003) were taken from Campbell and Norman (1998) and were 0.006 kg s m^{-3}, -0.7 J kg^{-1} and 1.7, respectively. These ψ_e and b values were consistent with measurements made in the laboratory on soil core samples collected from the experimental site (Elyn Humphreys, personal communication). For the 3 cm surface organic layer, values of K_S, ψ_e and b were 0.01 kg s m^{-3}, -0.1 J kg^{-1} and 1.7, respectively (Plamondon, 1972).

Our CO_2 diffusivity measurements were made for ε between 0.20 and 0.55 $m^3\,m^{-3}$ and were best described by Eq. (12) with $m = 0.93$ and $n = 0.56$, which we used in our model simulations.

The initial conditions were the measured profiles of soil temperature and water content, and an approximate profile of CO_2 concentration in soil air. For the boundary conditions at the bottom of the soil profile, gradients of soil water matric potential, temperature and CO_2 concentration were set to zero. Therefore the bottom of the soil profile was considered to be perfectly insulated for sensible heat but to allow gravitational drainage of water, and along with it some downward mass flow movement of dissolved CO_2. At the soil surface, a flux boundary condition was used for soil heat and water, while a concentration boundary condition was used for CO_2. The flux boundary conditions at the forest floor were the measured soil heat flux (G_S) and the rate of evaporation, which was approximated as 5% of the stand evapotranspiration (E) (Drewitt, 2002; Humphreys et al., 2003). The concentration boundary condition for soil CO_2 at the forest floor was the measured concentration obtained during the first 20 s of the 4 min closing of the automatic chambers used to measure soil CO_2 effluxes.

3.4. Numerical implementation of the model

Eqs. (1), (2) and (4) were solved, subject to the boundary conditions, using finite-difference techniques. Because of the highly non-linear relationships between hydraulic properties and soil water matric potential, the Newton-Raphson iterative method (Campbell, 1985) was used to solve Eq. (1). Eqs. (2) and (4) were solved using the Crank-Nicholson semi-implicit finite-difference method with an algorithm described by Richtmyer (1957). A distance step of 2 cm with a soil column depth of 1.5 m and a time step of 15 min were used in the calculations. The computer program for the numerical solutions, written in Matlab, version 5, used 4 min of clock time on a Pentium II desktop computer to do a 7-day simulation.

4. Results and discussion

4.1. Model validation

For the purpose of model validation, we used three 1-week periods, one in each of August, October and December 2000 to represent late summer through winter. These were selected mainly because the periods were rainless and the manual measurements of soil CO_2 concentrations were available. Using rainless periods to validate the model at this stage also helped avoid undue complexities such as rain interception by

the canopy, and displacement and/or compression of soil air.

Due to the sparseness of the mosses and very low light levels at the forest floor, the daytime photosynthetic uptake of CO_2 was generally negligible; however, chambers 4 and 5 showed measurable differences in their daytime and nighttime CO_2 efflux–temperature relationships (Drewitt et al. (2002). Daytime effluxes in these two chambers were lower by up to 9 and 8%, respectively. When averaged over the six chambers, the effect of moss photosynthesis on the CO_2 efflux measurement was less than 3%, and thus the average measured effluxes were assumed to be soil respiration. To better account for the spatial variability of CO_2 effluxes, we used data from all six chambers.

Figs. 1–3 show that the modeled soil CO_2 effluxes, temperatures and soil water contents agreed well with those measured in the field. CO_2 effluxes varied from about 10 μmol m^{-2} s^{-1} in August to as low as 2 μmol m^{-2} s^{-1} in December, decreasing as soil temperatures decreased. Diurnal variations of CO_2 efflux also followed variations of soil temperature, especially at the 2 cm depth, thereby indicating that the efflux followed the pattern of CO_2 production in the soil as determined mainly by soil temperature. Modeled half-hourly effluxes were always approximately equal to the modeled total production of CO_2 in the soil profile (to be discussed latter). Fig. 3 shows that from 11 December onwards the measured effluxes and soil water contents at the 2 cm depth were lower than modeled values. This happened because of freezing in the top few centimeters of soil, the air temperature during this period being below $-1\,^{\circ}C$. However, this was not evident in the measured and modeled temperatures, and, therefore, in modeled effluxes. This indicates the importance of accurate estimation of soil temperatures for modeling soil CO_2 production and transport.

Fig. 4 compares modeled CO_2 concentrations at the 20 cm depth with those measured at the same depth using the solid-state infrared carbon dioxide sensor during 25 September to 27 November 2002. The soil temperature and water content time series support the

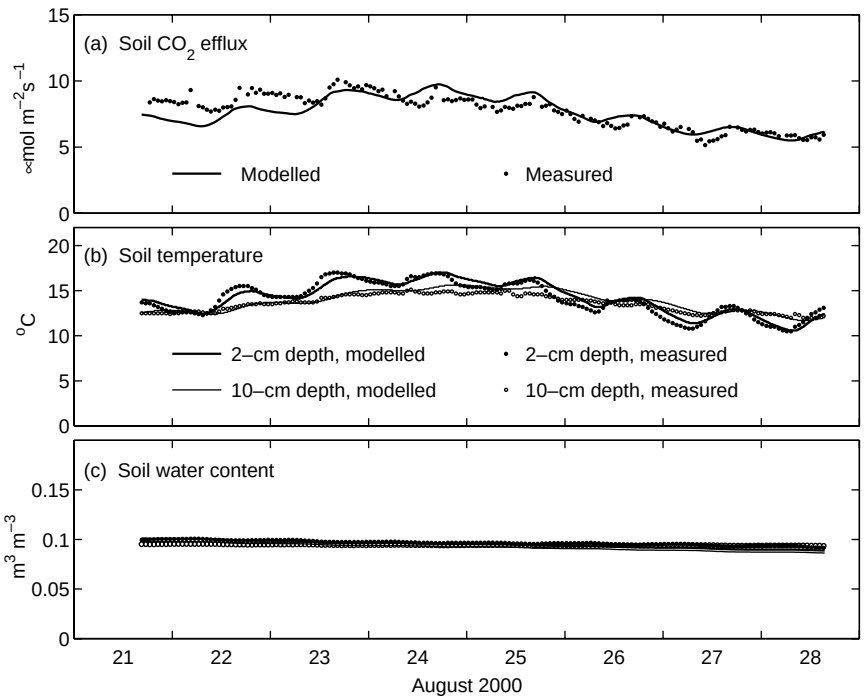

Fig. 1. Time series of measured and modeled soil CO_2 efflux, soil water content and temperature for an 8-day period of 21–28 August 2000 for the 54-year-old Douglas-fir forest floor at Campbell River, Vancouver Island, Canada. Measured soil CO_2 efflux data are averages from six chambers.

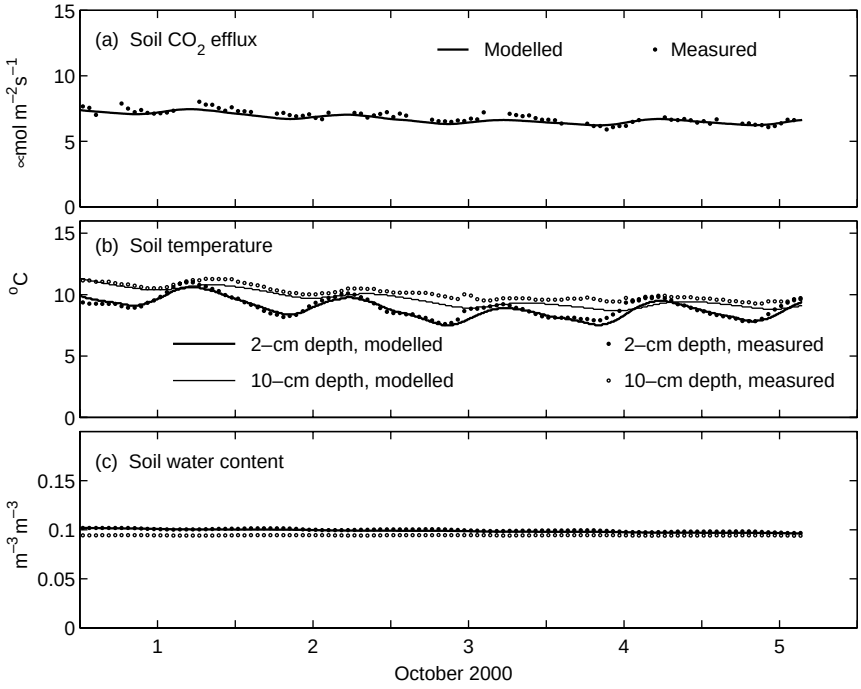

Fig. 2. Time series of measured and modeled soil CO_2 efflux, soil water content and temperature for a period of 1–5 October 2000 for the 54-year-old Douglas-fir forest floor at Campbell River, Vancouver Island, Canada. Measured soil CO_2 efflux data are averages from six chambers.

earlier observation that variations in soil CO_2 concentration are determined mainly by soil temperature variation. Nevertheless, an interesting feature of these results is that when the soil was very dry, a small increase, as little as 1%, in soil water content in the top few centimeters following rain on 3 October and 19 October, led to an unexpectedly large increase in measured soil CO_2 concentration at the 20 cm depth. This could not be accounted for by a decrease in diffusivity or a small increase in CO_2 production as determined by the $\alpha(\theta)$ function in the model. The most probable explanation for the increase is a sudden flush in soil microbial activity with a small increase in soil water content in a dry soil. Abrasimova (1979) reported a higher respiratory activity at a soil water content obtained by adding water to a dry soil than when the same water content was achieved by drying a saturated soil sample. Furthermore, it was difficult to match the modeled and measured soil water contents following rain (Fig. 4c). A possible explanation for this is the prevalence of 'bypass flow' of water in the macropores comprising old dead root channels, which would remove rain water faster than for flow in the soil matrix (Beven and Germann, 1982).

There was good agreement between measured and modeled soil CO_2 concentration profiles (Fig. 5), though measured values near the soil surface were slightly lower than modeled values. This may be partly due to ventilation by wind. Widen and Majdi (2001) observed significant effects of wind speed on the CO_2 concentration 3 cm beneath the organic layer in a mixed pine and spruce forest. Measurements by Hirsch et al. (2002) in a boreal forest floor, with high porosity near the surface, showed that wind turbulence significantly affected the near-surface soil CO_2 concentrations. High soil CO_2 concentrations, up to 10,000 μmol mol^{-1} in summer, decreasing to 6000 μmol mol^{-1} in winter, occurred at the 1 m depth in this forest soil. The existence of measurable concentration gradients at the 1 m depth indicates the occurrence of some CO_2 production, probably associated with very low diffusivities, at deeper depths.

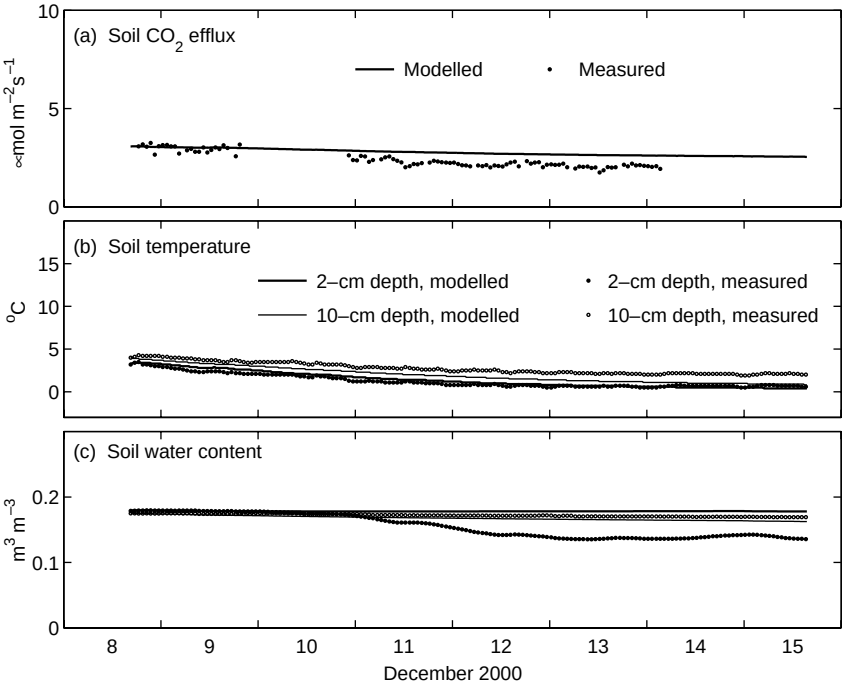

Fig. 3. Time series of measured and modeled soil CO_2 efflux, soil water content and temperature for a period of 8–15 December 2000 for the 54-year-old Douglas-fir forest floor at Campbell River, Vancouver Island, Canada. Measured soil CO_2 efflux data are averages from six chambers.

Fig. 6a shows the modeled soil CO_2 production profiles at the same times as the CO_2 concentration profiles shown in Fig. 5 were measured. Seasonal changes in soil CO_2 production followed the pattern of changes in near-surface soil temperature. For example, the highest and lowest production values occurred in September and December, respectively, corresponding to the highest and lowest 2 cm soil temperatures of 13 and 2 °C, respectively. Modeled C removal by root water uptake as well as that removed by water drainage was always less than 1% of the total production. Soil CO_2 diffusivity (Fig. 6c) decreased with soil depth and varied with season, the changes resulting from changes in air porosity (Fig. 6b) as determined from measured soil bulk density and soil water content. The diffusivity values for this forest floor varied from a high value of 7 $mm^2\,s^{-1}$ at the soil surface to less than 2 $mm^2\,s^{-1}$ at the 50 cm depth. These are similar to the measured diffusivities for a sandy loam forest soil at 20 °C reported by Hasimoto and Suzuki (2002). Fig. 7 shows how the modeled soil CO_2 flux varies with soil depth and season, the variation being less pronounced at deeper depths due to less production, and because soil temperature, water content and diffusivity vary little at deeper depths. The different flux–depth curves show that more than half of the total soil CO_2 efflux originated in the top 10 cm soil, corresponding to the R_{soil} profiles (Fig. 6).

Measured and modeled CO_2 effluxes shown in Figs. 1–3, and measured and modeled soil CO_2 concentrations shown in Fig. 5 agreed very well (Fig. 8). Modeled effluxes and soil CO_2 concentrations were within ±10% of measured values, which, in view of a large number of soil and environmental variables involved and the precision of their measurement, especially in forest soils, suggests good performance by the model.

4.2. Effects of soil water content

The model was used to investigate the effects of soil water content on soil CO_2 production, efflux and CO_2

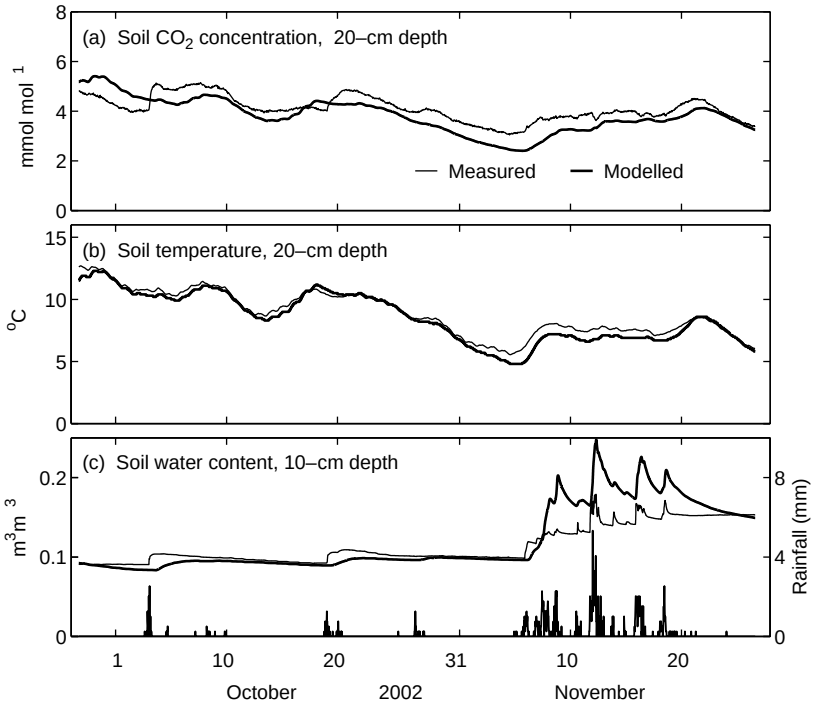

Fig. 4. Time series of measured and modeled soil CO_2 concentrations and temperatures at the 20 cm depth and soil water contents at the 10 cm depth. Soil CO_2 concentrations were measured with a solid-state infrared CO_2 sensor (Vaisala GMM221).

concentration. With all other inputs kept the same as in Fig. 1, soil water content was varied by simulating rainfall at $5\,mm\,h^{-1}$ for 6 h three times during the 7-day period. Following the rain events, efflux departed from total CO_2 production, only to catch up with it within a few hours, and was always within 5% of the total CO_2 production (Fig. 9). Both soil water content and soil CO_2 concentration increased following each rainfall event. The increase in efflux following the first rainfall is due to the increase in CO_2 production governed by the $\alpha(\theta)$ function. Subsequent rainfalls did not affect CO_2 efflux because the resulting changes in soil water content could not affect CO_2 production. Similar results were obtained when the rainfall intensity was increased to $10\,mm\,h^{-1}$ resulting in slightly higher soil water content and CO_2 concentration. It may be pointed out that soil water content at depths up to 1 m does not normally exceed 50% saturation as rain water drains rapidly in this coarse-textured soil (see Fig. 4). We also studied rain effects when the same soil organic matter and roots were distributed to deeper depths, most below 10 cm, and found very similar results. This shows that the half-hourly effluxes were well approximated by the total CO_2 production. This was because CO_2 diffusion in this forest soil was relatively rapid compared to changes in the rates of CO_2 production. This can also be shown by calculating the time for a CO_2 molecule to travel through a soil layer. For a molecule undergoing Brownian motion in a one-dimensional path, its root mean square displacement at time t is calculated following probability distribution considerations to be $\sqrt{2Dt}$ (Bard and Faulkner, 1980), where D is the molecular diffusivity. Thus in one-dimensional diffusive transport, the time, t, that it takes for a CO_2 molecule to diffuse along an actual path length, l, is given by $(l^2/2D_G)$. Substituting for D_G using Eq. (11) and recognizing that f_G is the ratio of the straight-line distance (d) to the actual path length (l) transversed by a molecule in a porous medium, the transit time becomes $(\varepsilon d^2/2f_G D_{CG})$. Winston et al. (1997) also used this equation to calculate transit time of CO_2 through soil and snow; however, they used

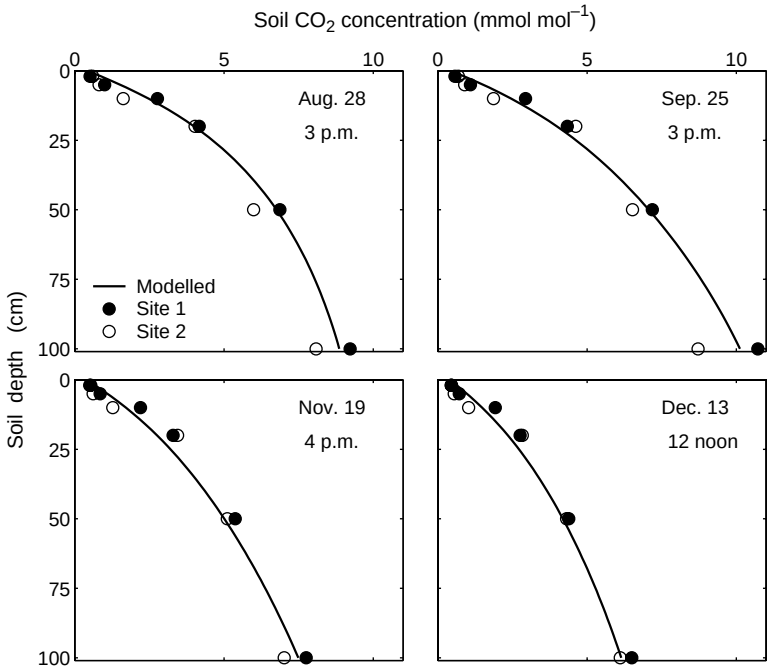

Fig. 5. Comparison of measured and modeled CO_2 concentrations in soil air when measurements were made during each of the four study periods. All times are in Pacific Standard Time (PST).

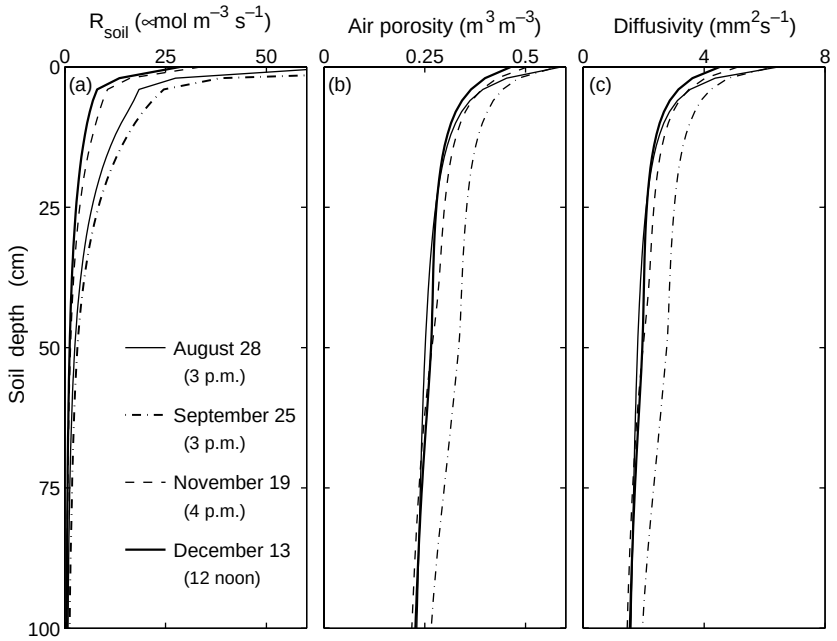

Fig. 6. Modeled soil CO_2 production (R_{soil}), air porosity and CO_2 diffusivity profiles for the times shown in Fig. 5.

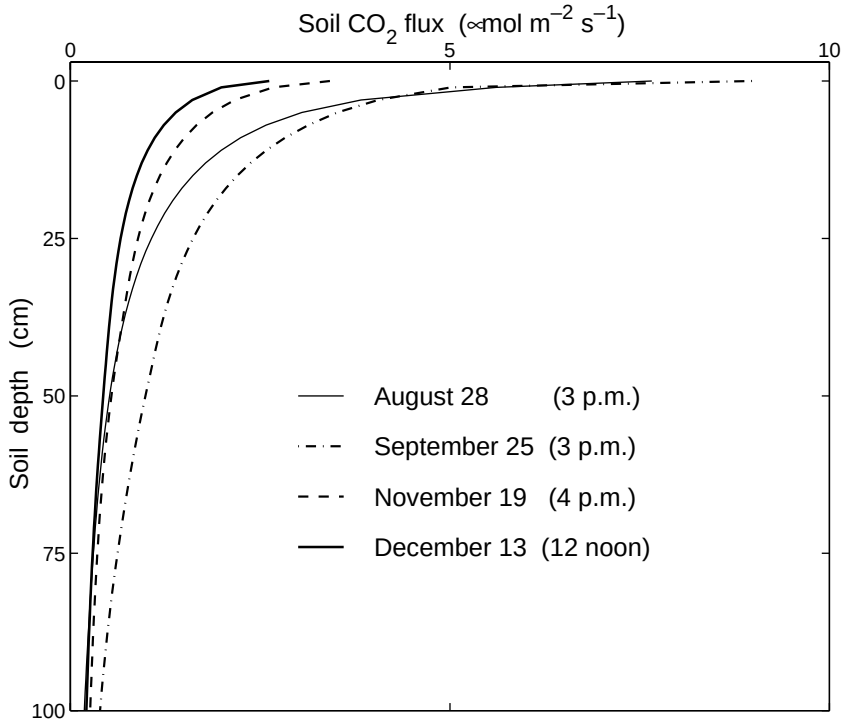

Fig. 7. Effect of soil depth and season on modeled upward soil CO_2 flux for the times shown in Fig. 5.

$f_G = 1$. Recalling that most of the CO_2 is produced in the top 20 cm soil (Fig. 6), and using $D_{CG} = 3\,mm^2\,s^{-1}$ and soil air-filled porosity, $\varepsilon = 0.3\,m^3\,m^{-3}$ (so that $f_G = 0.55$ from Eq. (12)), the time required for a molecule to travel through the 20 cm thick soil layer is less than an hour. Thus the time lag between CO_2 production and its escape from the soil surface, in general, should not be more than a few hours.

As the CO_2 diffusion coefficient in the liquid phase is about 10^{-4} times that in the gaseous phase, CO_2 diffusion in the liquid phase is usually considered negligible under most soil water conditions observed in the field. Simunek and Suarez (1993) assumed that the relation between f_L and θ is the same as between f_G and ε given by Millington and Quirk (1961), and showed that contributions from liquid-phase diffusion and gaseous-phase diffusion are equal when the relative air-filled porosity ($\varepsilon_R = \varepsilon/\theta_S$) is about 0.06. However, the relative contribution in the two phases will be dependent on the pH of the soil solution, which affects C_L/C_G as shown in Eq. (8). Following Simunek and Suarez's (1993) treatment of f_L and f_G, the ratio of fluxes from liquid-phase diffusion to gaseous-phase diffusion, for still water, is

$$\frac{F_L}{F_G} = \frac{D_L C_L}{D_G C_G}\left(\frac{\varepsilon_R}{1-\varepsilon_R}\right)^{-3.33} \quad (20)$$

Calculations with Eq. (20) in conjunction with Eq. (8) show that in the acidic to neutral pH range, contribution of liquid-phase flux will be negligible when relative air-filled porosity is greater than 0.12.

4.3. Discussion

This study describes the development of a simplified CO_2 production model and its coupling to the simultaneous transport of soil water, heat and CO_2. The model has been validated against measured soil CO_2 effluxes and CO_2 concentration profiles in a 54-year-old Douglas-fir forest, using independently determined model parameters. The model was capable of satisfactorily describing the diurnal as well as

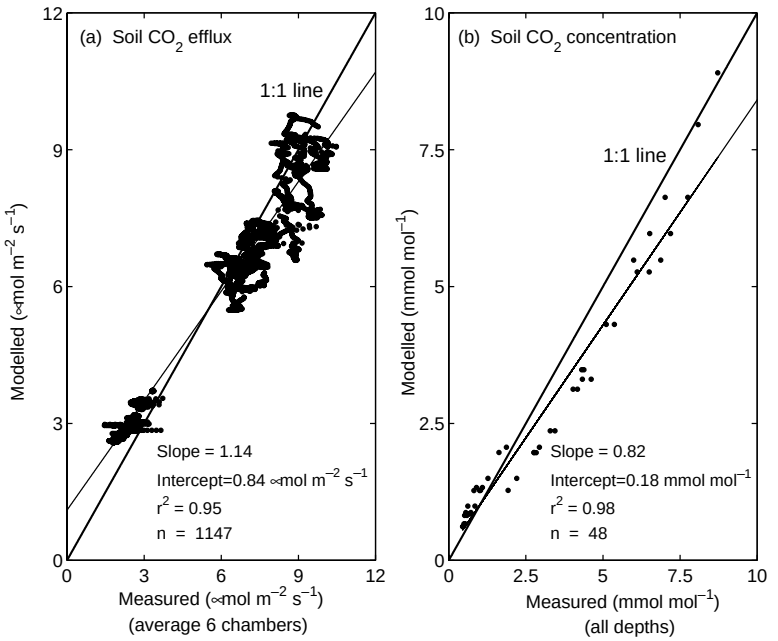

Fig. 8. Comparison of (a) measured and modeled soil CO_2 effluxes shown in Figs. 1–3 and (b) measured and modeled soil CO_2 concentrations shown in Fig. 5. The thin lines are the linear least-squares best fit to the data.

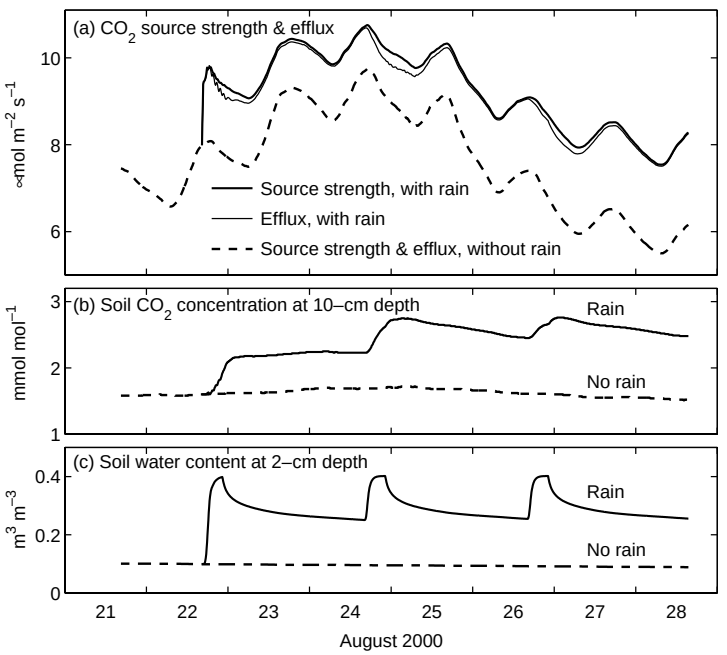

Fig. 9. Modeled time series of CO_2 source strength and efflux (a), soil CO_2 concentration (b) and soil water content (c), as influenced by rain events. Rainfall intensity was 5 mm h^{-1} and each event lasted for 6 h. All other inputs were the same as in Fig. 1.

seasonal variations in soil temperature and soil water content, which determine the production of CO_2 in the soil. Thus an accurate model of soil temperature and water content is essential in modeling soil CO_2 efflux.

A wide range of Q_{10} values, varying with season and soil depth and different for mineral soil and roots, have been often reported (e.g. Anderson, 1973; Boone et al., 1998; Drewitt et al., 2002; Fang and Moncrieff, 2001; Widen and Majdi, 2001; Winkler et al., 1996). These estimates come from efflux measurements made under different soil, plant and environmental conditions; however, they invariably refer to a single near-surface soil temperature only while the production of CO_2 takes place in the entire biologically active soil profile. We found that the widely accepted value of 2 for Q_{10} for the bulk mineral soil and 4 (Witkamp, 1969) for the surface organic layer resulted in a better agreement with the measured soil CO_2 effluxes as well as soil CO_2 concentrations.

In this study, soil respiration was assumed to be well approximated by the CO_2 efflux measured by transparent chambers. This was possible because photosynthesis and respiration by mosses and shrubs had a negligible (<3%) effect on soil CO_2 efflux. In ecosystems with significant moss and shrubs, it is necessary to use darkened chambers as well as to account for the respiration rates of these plants in order to determine soil respiration. In order to apply the model described in this study to such ecosystems, it will be necessary to include moss photosynthesis and respiration.

5. Conclusions

1. This simplified CO_2 production model coupled to simultaneous transport of soil water, heat and CO_2 satisfactorily described the diurnal and seasonal variations in forest floor CO_2 efflux as well as soil temperature, water content and CO_2 concentration profiles. The efflux was most sensitive to soil temperature, and the influence of soil water content was relatively small.
2. In this rapidly draining soil, the CO_2 efflux, even at time scales as short as an hour, was very well approximated by the total production of CO_2 in the soil profile, even during and after rainfalls, which significantly increased soil water content. This occurred because CO_2 diffusion in the soil was relatively rapid compared to changes in the rates of CO_2 production in the forest soil.
3. In this podzolic soil ecosystem with low soil pH and rapid drainage, liquid-phase diffusion is unlikely to play a major role in CO_2 transport.
4. High soil CO_2 concentrations, up to 10,000 μmol mol^{-1} in summer and 6000 μmol mol^{-1} in winter, and a positive downward gradient at the 1 m depth in this forest ecosystem indicate the occurrence of CO_2 production together with a very low CO_2 diffusivity at depths greater than 1 m.

Acknowledgements

This research was funded by the Canadian Foundation for Climate and Atmospheric Sciences (CFCAS) as a part of Development of a Canadian Global Coupled Carbon Climate Model (GC^3M) project, a Natural Sciences and Engineering Research Council (NSERC) operating grant, and the Fluxnet Canada Research Network (NSERC, CFCAS and BIOCAP Canada). We gratefully acknowledge the thoughtful comments by two anonymous referees, which greatly helped to improve the quality of the manuscript.

References

Abrasimova, L.N., 1979. Hysteresis and temperature dependence of O_2 and CO_2 gas exchange processes in soils (Russian, English summary). Pochvovedenie 6, 86–91.

Anderson, J.M., 1973. Carbon dioxide evolution from two temperate, deciduous woods and soils. J. Appl. Ecol. 10, 361–378.

Bard, A.J., Faulkner, L.R., 1980. Electrochemical Methods. Wiley, New York.

Beven, K., Germann, P., 1982. Macropores and water flow in soils. Water Resour. Res. 18, 1311–1325.

Boone, R.D., Nadelhoffer, K.J., Canary, J.D., Kaye, J.P., 1998. Roots exert a strong influence on the temperature sensitivity of soil respiration. Nature 396, 570–572.

Bunnell, F.L., Tait, D.E.N., Flanagan, P.W., vanCleve, K., 1977. Microbial respiration and substrate weight loss. I. A general model of the influence of abiotic variables. Soil Biol. Biochem. 9, 33–40.

Burton, A.J., Pregitzer, K.S., Zogg, G.P., Zak, D.R., 1998. Drought reduces root respiration in sugar maple forests. Ecol. Appl. 8, 771–778.

Campbell, G.S., 1985. Soil Physics with BASIC. Springer-Verlag, New York, 150 pp.

Campbell, G.S., Norman, J.M., 1998. An Introduction to Environmental Biophysics. Springer-Verlag, New York, 286 pp.

Chapman, S.B., 1979. Some interrelationships between soil and root respiration in lowland Colluna heathland in southern England. J. Ecol. 67, 1–20.

Currie, J.A., 1965. Diffusion within the soil microstructure—a structural parameter for soils. J. Soil Sci. 16, 279–289.

Drewitt, G.B., 2002. Carbon dioxide flux measurements from a coastal Douglas-fir forest. Unpublished Ph.D. Thesis, University of British Columbia, Vancouver, BC.

Drewitt, G.B., Black, T.A., Nesic, Z., Humphreys, E.R., Jork, E.M., Swanson, R., Ethier, G.J., Griffs, T., Morgenstern, K., 2002. Measuring forest floor CO_2 fluxes in a Douglas-fir forest. Agric. For. Meteorol. 110, 299–317.

Fang, C., Moncrieff, J.B., 1999. A model of CO_2 production and transport. 1. Model development. Agric. For. Meteorol. 95, 225–236.

Fang, C., Moncrieff, J.B., 2001. The dependence of soil CO_2 efflux on temperature. Soil Biol. Biochem. 33, 155–165.

Gerwitz, A., Page, E.R., 1974. An empirical mathematical model to describe plant root systems. J. Appl. Ecol. 11, 773–781.

Glinski, J., Stepniewski, W., 1985. Soil Aeration and its Role for Plants. CRC Press, Boca Raton, FL, 229 pp.

Goulden, M.L., Munger, J.W., Fan, S.M., Daube, B.C., Wolfsy, S.C., 1996. Measurements of carbon sequestration by long-term eddy covariance: methods and critical evaluation of accuracy. Global Change Biol. 2, 169–182.

Grier, C.C., Vogt, K.A., Keys, M.R., Edmonds, R.L., 1981. Biomass distribution and above- and below-ground production in young and mature *Abies amabilis* zone ecosystems of the Washington Cascades. Can. J. For. Res. 11, 155–167.

Hanson, P.J., Wullschleger, S.D., Bohlan, S.A., Todd, D.E., 1993. Seasonal and topographic patterns of forest floor CO_2 efflux from an upland oak forest. Tree Physiol. 13, 1–15.

Harned, H.S., Davies Jr., R., 1943. The ionization constants of carbonic acid in water and the solubility of carbon dioxide in water and aqueous salt solutions from 0 to 50°. J. Am. Chem. Soc. 65, 2030–2065.

Hasimoto, S., Suzuki, M., 2002. Vertical distribution of carbon dioxide diffusion coefficients and production rates in forest soils. Soil Sci. Soc. Am. J. 66, 1151–1158.

Hirsch, A.I., Trumbore, S.E., Goulden, M.L., 2002. Direct measurement of the deep soil respiration accompanying seasonal thawing of a boreal forest soil. J. Geophys. Res. 108, 1–10.

Hook, W.R., Livingston, N.J., 1996. Errors in converting time domain reflectometry measurements of propagation velocity to estimates of soil water content. Soil Sci. Soc. Am. J. 60, 35–41.

Humphreys, E.R., Black, T.A., Ethier, G.J., Drewitt, G.B., Spittlehouse, D.L., Jork, E.M., Nesic, Z., Livingston, N.J., 2003. Annual and seasonal variability of sensible and latent heat fluxes above a coastal Douglas-fir forest, British Columbia, Canada. Agric. For. Meteorol. 115, 109–125.

Janssens, I.A., Lankreijer, H., Matteucci, G., Kowalski, A.S., Buchman, N., Epron, D., Pilegaard, K., Kutsch, W., Longdoz, B., Grunwald, T., Montagnani, L., Dore, S., Rebmann, C., Moors, E.J., Grelle, A., Rannik, U., Morgenstern, K., Oltchev, S., Clement, R., Gudmundsson, J., Minerbi, S., Berbigier, P., Ibrom, A., Moncrieff, J., Aubinet, M., Bernhofer, C., Jensen, N.O., Vesala, T., Granier, A., Schulze, E.D., Lindroth, A., Dolman, A.J., Jarvis, P.G., Ceulamans, R., Valentini, R., 2001. Productivity overshadows temperature in determining soil and ecosystem respiration across European forests. Global Change Biol. 7, 269–278.

Jassal, R.S., Novak, M.D., Black, T.A., 2003. Effect of surface layer thickness on simultaneous transport of heat and water in a bare soil and its implications for land surface schemes. Atmos. Ocean 41, 259–272.

Kurz, W.A., 1989. Net primary production, production allocation, and foliage efficiency in second growth Douglas-fir stands with differing site quality. Unpublished Ph.D. Thesis, University of British Columbia, Vancouver, BC.

Law, B.E., Ryan, M.G., Anthony, P.M., 1999. Seasonal and annual respiration of a Ponderosa pine ecosystem. Global Change Biol. 5, 169–182.

Livingstone, G.P., Hutchinson, G.L., 1995. Enclouser-based measurements of trace gas exchange: applications and sources of error. In: Matson, P., Harriss, R. (Eds.), Biogenic Trace Gases: Measuring Emissions form Soil and Water. Blackwell Scientific, Oxford, UK, pp. 14–51.

Marshall, T.J., 1959. The diffusion of gases through porous media. J. Soil Sci. 10, 79–82.

Millington, R.J., Quirk, J.P., 1961. Permeability of porous solids. Trans. Faraday Soc. 57, 1–8.

Moncrieff, J.B., Fang, C., 1999. A model for soil CO_2 production and transport. 2. Applications to a Florida *Pinus elliotte* plantation. Agric. For. Meteorol. 95, 237–256.

Monreal, C.M., Zentner, R.P., Robertson, J.A., 1997. An analysis of soil organic matter dynamics in relation to management, erosion and yield of wheat in long-term crop rotation plots. Can. J. Soil Sci. 77, 553–563.

Muller, C., 2000. Modelling Soil–Biosphere Interactions. CAB International, Wallingford, Oxen, UK, 354 pp.

Nakane, K., 1994. Modelling the soil carbon cycle of pine ecosystems. Ecol. Bull. 43, 161–172.

Nielsen, D.R., vanGenuchten, M.T.H., Biggar, A.W., 1986. Water flow and solute transport processes in the unsaturated zone. Water Resour. Res. 22, 89S–108S.

Norman, J.M., Kucharik, C.J., Gower, S.T., Baldochhi, D.D., Crill, P.M., Rayment, M., Savage, K., Strriegl, R.G., 1997. A comparison of six methods of measuring soil-surface carbon dioxide fluxes. J. Geophys. Res. 102, 28771–28777.

Paul, E.A., Harris, D., Collins, H.P., Schulthess, U., Robertson, G.P., 1999. Evolution of CO_2 and soil carbon dynamics in biologically managed row-crop agroecosystems. Appl. Soil Ecol. 11, 53–65.

Plamondon, A.P., 1972. Hydrological properties and water balance of the forest floor of a Canadian west coast watershed. Unpublished Ph.D. Thesis, University of British Columbia, Vancouver, BC.

Pritchard, D.T., Currie, J.A., 1982. Diffusion coefficients of carbon dioxide, nitrous oxide, ethylene and ethane in air and their measurement. J. Soil Sci. 33, 175–184.

Raich, J.W., Schlesinger, W.H., 1992. The global carbon dioxide flux in respiration and its relationship to vegetation and climate. Tellus 44B, 81–99.

Rayment, M.B., Jarvis, P.G., 2000. Temporal and spatial variation of soil CO_2 efflux in a Canadian boreal forest. Soil Biol. Biochem. 32, 35–45.

Richtmyer, R.D., 1957. Difference Methods for Initial Value Problems. Interscience, New York, pp. 101–104.

Robinson, R.A., Stokes, R.H., 1959. Electrolyte Solutions. Butterworths, London.

Simunek, J., Suarez, D.L., 1993. Modelling carbon dioxide transport and production in soil. 1. Model development. Water Resour. Res. 29, 487–497.

Steele, S.J., Gower, S.T., Vogel, J.G., Norman, J.M., 1997. Root mass, net primary production and turnover in aspen, jack pine and black spruce forests in Saskatchewan and Manitoba, Canada. Tree Physiol. 17, 577–587.

Stumm, W., Morgan, J.J., 1981. Aquatic Chemistry: An Introduction Emphasizing Chemical Equilibria in Natural Waters. Wiley, New York.

Tesarova, M., Gloser, J., 1976. Total CO_2 output from alluvial soils with two types of grassland communities. Pedobiologia 16, 364–372.

Tinker, P.B., Nye, P.H., 2000. Solute Movement in the Rhizosphere. Oxford University Press, UK, 444 pp.

vanVeen, J.A., Paul, E.A., 1981. Organic carbon dynamics in grassland soils. I. Background information and computer simulation. Can. J. Soil Sci. 61, 185–201.

Wang, H., Curtin, D., Jame, Y.W., McConkey, B.G., Zhou, H.F., 2002. Simulation of soil carbon dioxide flux during plant residue decomposition. Soil Sci. Soc. Am. J. 66, 1304–1310.

Widen, B., Majdi, H., 2001. Soil CO_2 efflux and root respiration at three sites in a mixed pine and spruce forest: seasonal and diurnal variations. Can. J. For. Res. 31, 786–796.

Winkler, J.L., Cherry, R.S., Schlesinger, W.H., 1996. The Q_{10} relationship of microbial respiration in a temperate forest soil. Soil Biol. Biochem. 28, 1067–1072.

Winston, G.C., Sundquist, E.T., Stephens, B.B., Trumbore, S.E., 1997. Winter CO_2 fluxes in a boreal forest. J. Geophys. Res. 102 (D24), 795–804.

Witkamp, M., 1969. Cycles of temperature and carbon dioxide evolution from litter and soil. Ecology 50, 922–924.